A Technique for Evaluation of CCD Video-Camera Noise

Kenji Irie, *Member, IEEE*, Alan E. McKinnon, Keith Unsworth, and Ian M. Woodhead, *Member, IEEE*

***Abstract*—This paper presents a technique to identify and measure the prominent sources of sensor noise in commercially available charge-coupled device (CCD) video cameras by analysis of the output images. Noise fundamentally limits the distinguishable content in an image and can significantly reduce the robustness of an image processing application. Although sources of image sensor noise are well documented, there has been little work on the development of techniques to identify and quantify the types of noise present in CCD video-camera images. A comprehensive noise model for CCD cameras was used to evaluate the technique on a commercially available CCD video camera.**

***Index Terms*—Charge-coupled devices (CCDs), image processing, noise measurement, video signal processing.**

I. Introduction

ADVANCEMENTS in digital image sensors have led to the wide use of digital cameras in image processing applications. Many of these applications attempt to extract useful information from the images, which is fundamentally limited by their signal-to-noise ratio (SNR). Although sources of image noise are well documented there has been little work on the assessment and validation of these noise sources by experimentation and analysis. This study presents a technique for the measurement of charge-coupled device (CCD) video-camera noise components based upon measurement of output images alone. A complete model of CCD camera noise is required to quantify and validate the technique.

II. CCD Camera Noise Model

An overview of the CCD architecture pertinent to this study is available in [1]. Using that architecture, we define and segment noise into the functional categories of spatially fixed, temporally varying, and digital processing for the purpose of experimental measurement. The complete CCD camera noise model was derived from existing research into the various sources of camera noise [1]–[7]. Each noise source is given in Tables I–III, and the complete noise model shown in Fig. 1. Given a fixed CCD-sampling frequency all sources are considered additive Gaussian distributed [3], [8], [9]. From Fig. 1, the equation for noisy image capture N_{cap} is

$$\begin{aligned} N_{\text{cap}} = &(I \times PRNU + SN_{\text{ph}}(I) \\ &+ I + FPN + SN_{\text{dark}} + N_{\text{read}}) \\ &\times N_D \times N_{\text{filt}} + N_Q \end{aligned} \tag{1}$$

TABLE I
Illumination-Independent Noise Types

Noise type	Origin	Manifestation	Dependencies
N_R, reset noise.	CCD support IC.	Additive temporal and spatial variance.	Temperature.
N_{therm}, combined thermal noise.	CCD support IC's.	Additive temporal and spatial variance.	Temperature.
N_{other}, combined flicker noise, transistor dark currents, and other minor contributors.	CCD sensor and CCD support IC's.	Additive temporal and spatial variance.	Temperature, CCD readout rate.
N_{read}, readout noise. Combined N_R+N_{therm}+N_{other}.	As per N_R, N_{therm}, and N_{other}.	Additive temporal and spatial variance.	Temperature, CCD readout rate.
SN_{dark}, dark-current shot noise.	CCD sensor.	Additive temporal and spatial variance.	Temperature, exposure time.
FPN, offset fixed-pattern noise.	CCD sensor.	Additive spatial variance only.	Temperature, exposure time.

TABLE II
Illumination-Dependent Noise Types

Noise type	Origin	Manifestation	Dependencies
PRNU, photo-response non-uniformity.	CCD sensor.	Multiplicative spatial variance only.	Incident pixel illumination.
SN_{ph}, photon shot noise.	CCD sensor.	Additive temporal and spatial variance.	Incident pixel illumination.

TABLE III
Digital Processing Noise Effects Types

Noise type	Origin	Manifestation	Dependencies
N_D, demosaicing noise.	CCD support IC.	Multiplicative noise amplification or attenuation.	Demosaicing implementation, combined sensor noise.
N_{filt}, post image-capture effects.	CCD support IC.	Multiplicative noise effect.	Parameters for image enhancement, combined sensor noise.
N_Q, quantization noise.	CCD support IC.	Additive noise. Image content dependent.	Variance of image data. Sets lower noise limit for non-trivial image content.

where I is the sensor irradiance. The camera's output-referred measurement of irradiance is the pixel value, measured as the mean pixel-value over an area of image or an image set.

III. Method of Noise Measurement

Video images of a GretagMacbeth ColorChecker Color Rendition Chart[1] (GMB) were taken with controlled fluorescent and incandescent lighting[2] and the chart was positioned to fill the image frame. A *Unibrain Fire-i400* color camera (Table IV) was defocused to reduce the effect of high-frequency content in the observed image that could affect the noise analysis. The illumination sources were positioned above the camera and directed

Manuscript received October 19, 2006; revised February 13, 2007 and March 30, 2007. This work was supported in part by the New Zealand Foundation for Research, Science, and Technology under Program LVLX0401. This paper was recommended by Associate Editor S. Takamura.

K. Irie and I. M. Woodhead are with Lincoln Ventures Ltd, Lincoln, Christchurch 7640, New Zealand (e-mail: iriek@lvl.co.nz; woodhead@lvl.co.nz).

A. E. McKinnon and K. Unsworth are with Lincoln University, Canterbury, New Zealand. (e-mail: mckinnon@lincoln.ac.nz, unsworth@lincoln.ac.nz).

Digital Object Identifier 10.1109/TCSVT.2007.913972

[1]http://www.gretagmacbeth.com

[2]Each light source was adjusted to provide similar camera RGB response for a gray-scale image.

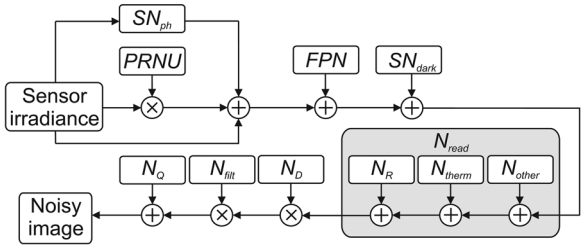

Fig. 1. Derived noise model for image capture in a standard CCD digital video camera.

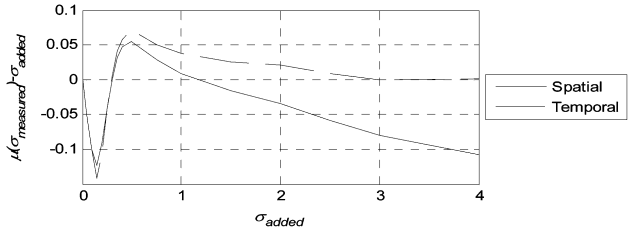

Fig. 2. Spatial and temporal quantization error curves for noisy, simulated images without a lighting source.

TABLE IV
UNIBRAIN FIRE I400 CAMERA DETAILS

Parameter	Value
Sensor type	Sony Wfine ICX098BQ ¼" color CCD (Bayer colour filter)
Native resolution	640 x 480
Video mode	24-bit RGB (8-bits per color channel)
Interface	IEEE-1394a (Firewire)

towards the chart such that the image was free from direct specular reflection. Simulated images were generated for the analysis of quantization and demosaicing effects.

An area of 50 pixels by 50 pixels was extracted from the centre of the image of each GMB gray-scale panel for analysis, and the camera was calibrated prior to measurement to remove any stuck or "hot" pixels. Experiments were performed at an ambient temperature of approximately 22 °C, where the CCD temperature was approximately 29 °C.

Methods for analysis of temporal noise, spatial noise, and total noise were formulated for each row and column of image data. The standard deviation (σ) was chosen as the measure of image noise as it can be easily related to the magnitude of pixel variations. The mean value of each panel, μ_p, taken as the mean of the extracted 50×50 panel, was used as a measure of I. For this study 100 images were used to achieve a 95% confidence interval for the resulting image analysis $(\sigma < 5)$ [9]. The following describes the method used to calculate each noise value:

1) Temporal noise, $\mu(\sigma_t)$.
   a) σ of temporal data, σ_t, for each pixel was calculated over the set of 100 images.
   b) σ_t for all pixels were then averaged, giving a value $\mu(\sigma_t)$ for the mean temporal variation for the panel.
2) Spatial (fixed-pattern) noise, $\sigma(\mu_t)$.
   a) The mean of the temporal data, μ_t, for each pixel was calculated over the set of 100 images.
   b) A second-order polynomial fit for each column of μ_t was calculated and subtracted from the data to remove optical effects such as vignetting and $1/R^2$ illumination fall-off expected from the use of a discrete illumination source.
   c) The residuals after subtraction of the polynomial-fitted data were concatenated and σ calculated to determine a value of $\sigma(\mu_t)$ for the mean spatial variation for the panel.
3) Total image noise, $\mu(\sigma_r)$, $\mu(\sigma_c)$.
   a) A second-order polynomial fit was calculated for each data row and column of an image of a GMB panel, and the fitted line was subtracted from the data to remove optical effects.
   b) The residuals after subtraction of each fitted line were concatenated and σ of the concatenated data calculated to give row and column noise values σ_r and σ_c, respectively.
   c) σ_r and σ_c for the panel were averaged over 100 test images to derive the final noise figures $\mu(\sigma_r)$ and $\mu(\sigma_c)$ for the panel for each image set.

In this work the camera's post-capture filters such as gamma, gain, white balance and contrast were disabled or set to neutral, and images were transferred in the RGB format, rendering N_{filt} as an identity function.

IV. RESULTS FROM SIMULATED IMAGES

A. Quantization Noise

It is common for images to be quantized for export from the camera (typically between 8–16 bits per channel). We have deduced that where the quantization step is very small compared to variations within the signal, the quantization process adds noise to the signal according to [10]

$$\hat{\sigma}^2_{\text{quantization}} = \frac{q^2}{12} \tag{2}$$

where q is the quantizing step. For $q = 1$

$$\hat{\sigma}_{\text{quantization}} = 0.29 \tag{3}$$

so that any data with significant variation will exhibit quantization noise up to $\sigma = 0.29$. However, many test images did not contain significant variations yet the effects of quantization need to be analyzed for such images. Hence, experiments were conducted to measure the effect of quantization using simulated images both with and without significant variations, using modeled point-source illumination to generate lighting variations in the form of lighting gradients.

Fig. 2 shows the results of quantization error from analysis of panel 19 using simulated GMB images with increasing additive Gaussian noise in dark conditions, using the methods for measuring spatial and temporal image noise described in Section III. As there is no significant variation in the image data (e.g., no lighting gradient, or visible scene data) there is an initial dip in the error curves caused by the rounding of noise to zero. Both spatial and temporal curves peak at $\sigma = 0.5$, where for values $\sigma > 0.5$ the temporal curve approaches zero and the spatial

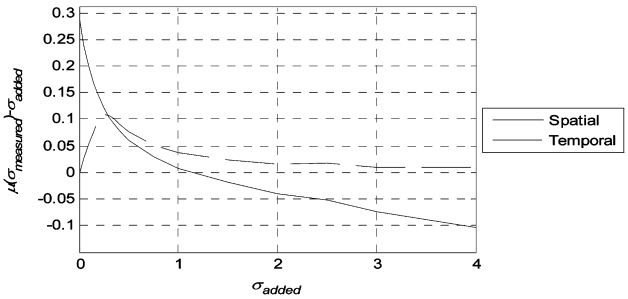

Fig. 3. Spatial and temporal quantization error curves for noisy, simulated images with point-source lighting.

curve continues a downward trend below zero due to the polynomial fitting to noise.

Fig. 3 shows the same analysis as for Fig. 2 but with the addition of simulated point-source lighting. This increases the dynamic range of the data by creating a gradient across the measured panel, reducing the significance of the quantization step for low additive noise values. This lighting gradient clearly affects spatial noise analysis as the nontrivial image data now exhibit a minimum noise level of $\sigma = 0.29$, as calculated in (3). Temporal noise measurement is also affected with continual over-estimation of the real noise level. Both curves exhibit similar responses to those in Fig. 2 for added noise values $\sigma > 0.5$.

For each experiment utilizing quantization noise, N_q, the appropriate quantization noise curve illustrated in Figs. 2 and 3 was used (temporal or spatial, lighting gradient or nonlighting gradient).

B. Demosaicing

The effect of demosaicing on image noise was analyzed and tested by measuring noise levels on simulated sets of GMB color chart images. However, there are many methods for demosaicing the Bayer array [11] and the method used in the i400 camera was unknown. A bilinear interpolation (BL) method was assumed, as images from the camera exhibit similar zipper-type artifacts along the vertical and horizontal edges in the simulated images generated using the BL method. The Bayer array measures the green image on a quincunx grid and the red and blue images on a rectangular grid. Half of the green pixels and three quarters of the red and blue pixels are interpolated. For the BL demosaicing method the interpolated green pixels are derived from four surrounding measured green pixels. Assuming that individual pixel noise values are independent

$$\hat{\sigma}_{\mathrm{interp},G} = \sqrt{\left(\frac{\sigma_G}{4}\right)^2 + \left(\frac{\sigma_G}{4}\right)^2 + \left(\frac{\sigma_G}{4}\right)^2 + \left(\frac{\sigma_G}{4}\right)^2} = \frac{\sigma_G}{2}. \quad (4)$$

The effect of BL demosaicing on the green channel noise is given by analysis of the entire green channel (50% interpolated), giving the total green-channel demosaiced noise attenuation

$$\hat{\sigma}_{\mathrm{demosiac},G} = \frac{1}{2}\left(\sigma_G + \frac{\sigma_G}{2}\right) = 0.75\sigma_G. \quad (5)$$

In each BL demosaiced image one quarter of red and blue pixels are interpolated from four surrounding measured pixels, and half of the red and blue pixels are interpolated from two surrounding pixels, depending on their location within the Bayer matrix. For the entire red channel

$$\hat{\sigma}_{\mathrm{demosaic},R} = \frac{1}{4}\left(\sigma_R + \sqrt{2}\sigma_R + \frac{\sigma_R}{2}\right) = 0.73\sigma_R. \quad (6)$$

Similarly, for the entire blue channel:

$$\hat{\sigma}_{\mathrm{demosaic},B} = 0.73\sigma_B. \quad (7)$$

To verify the above, a series of noisy simulated images was generated with added Gaussian noise levels from $\sigma = 0$ to 5, a range empirically determined by observation of noise levels across several CCD cameras. The removal of quantization effects results in an approximately linear noise response, and measurement of the gradients of the demosaiced noise curves provides the BL demosaicing values for spatial and temporal noise analysis shown in Table V.

TABLE V
MEASURED ATTENUATION OF BAYER-ARRAY BILINEAR INTERPOLATION

Measured noise	Spatial	Temporal
$\sigma_{\mathrm{demosaic},R}$	$0.71\sigma_R$	$0.73\sigma_R$
$\sigma_{\mathrm{demosaic},G}$	$0.77\sigma_G$	$0.75\sigma_G$
$\sigma_{\mathrm{demosaic},B}$	$0.71\sigma_B$	$0.73\sigma_B$

V. RESULTS FROM RECORDED IMAGES

A. Offset FPN

FPN was measured by analyzing a set of images taken in dark conditions with no illumination (n.i.). Equation (1) becomes

$$N_{\mathrm{n.i.}} = (FPN + SN_{\mathrm{dark}} + N_{\mathrm{read}}) \times N_D + N_Q. \quad (8)$$

The temporal averaging of images effectively removes the terms SN_{dark} and N_{read} giving

$$N_{n.i.,\mathrm{avg}} = FPN \times N_D + N_Q. \quad (9)$$

Subtracting N_Q from (9) and dividing by N_D leaves *FPN*. The measured *FPN* noise for the i400 camera was taken as being the mean measured value of $(\sigma(\mu_t) - N_Q/N_D)$ for each channel

$$\begin{aligned} FPN_R &= 0.300 \\ FPN_G &= 0.123 \\ FPN_B &= 0.247. \end{aligned} \quad (10)$$

B. Dark Current Shot Noise and Readout Noise

SN_{dark} is generated within the photodetector and is dependent upon the leakage photocurrent. The value of dark-current shot noise voltage can be sampled at the end of photocurrent integration, where the mean square value of noise voltage is proportional to the integration (exposure) time [6].

Equation (8) gives the measurable noise component given no illumination. Taking the temporal variations over the set of images removes FPN, giving combined dark-shot and read noise

$$N_{\mathrm{n.i.,t}} = (SN_{\mathrm{dark}} + N_{\mathrm{read}}) \times N_D + N_Q \quad (11)$$

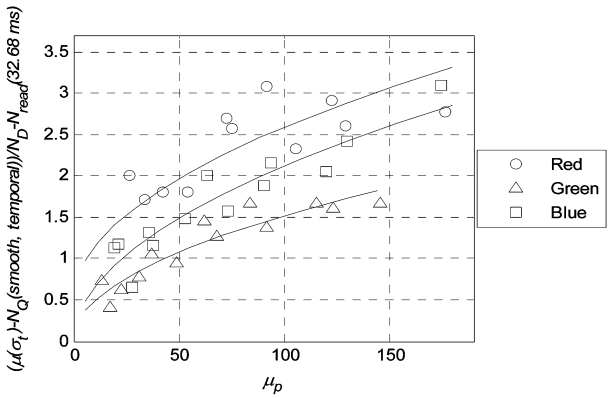

Fig. 4. Measured $SN_{\rm ph}$ for the i400 camera.

where $N_{\rm n.i.,t}$ is the temporal noise without illumination. Subtracting N_Q and dividing by N_D gives $SN_{\rm dark} + N_{\rm read}$. As $SN_{\rm dark}$ is a function of exposure, a value of $N_{\rm read}$ can be determined by extrapolation to zero of the temporal noise curve. Like FPN, the shape of the $SN_{\rm dark} + N_{\rm read}$ noise curves was effectively flat showing no apparent trend of increasing noise with exposure, suggesting that $SN_{\rm dark}$ is swamped by readout noise which effectively removes $SN_{\rm dark}$ from the noise model for the i400 camera. The measured $N_{\rm read}$ was taken as the mean measured value of $(\mu(\sigma_t) - N_Q/N_D)$ for each channel

$$\begin{aligned} N_{{\rm read},R} &= 1.612 \\ N_{{\rm read},G} &= 0.613 \\ N_{{\rm read},B} &= 1.240. \end{aligned} \tag{12}$$

C. Photon Shot Noise

For a given illumination, measurement of temporal values only in (1) removes I along with spatial noise terms FPN and $PRNU$ giving

$$N_t = (SN_{\rm ph}(I) + SN_{\rm dark} + N_{\rm read}) \times N_D + N_Q. \tag{13}$$

Photon shot noise, $SN_{\rm ph}$, can be measured by subtracting N_Q, dividing by N_D, then subtracting the previously measured $SN_{\rm dark}$ (zero for the measured camera) and $N_{\rm read}$. Fig. 4 shows photon shot-noise for images captured at maximum exposure (32.68 ms) with different illumination intensities for the i400 camera. A slight trend can be seen in each of the color channels that has noise $\approx \mu_p^{0.5}$ as expected from the Poisson sampling theorem for sampling of discrete quanta. A square-root curve was fitted for each color giving the equation for measured $SN_{\rm ph}$

$$\begin{aligned} SN_{ph,R} &= 0.212\sqrt{\mu_{p,R}} + 0.468 \\ SN_{ph,G} &= 0.515\sqrt{\mu_{p,G}} + 0.009 \\ SN_{ph,B} &= 0.215\sqrt{\mu_{p,B}} - 0.040 \end{aligned} \tag{14}$$

D. PRNU

Measurement of spatial variations removes I and any temporal terms from (1) giving the value for spatial noise without filtering (s,n.f.):

$$N_{\rm s,n.f} = (I \times PRNU + FPN) \times N_D + N_Q. \tag{15}$$

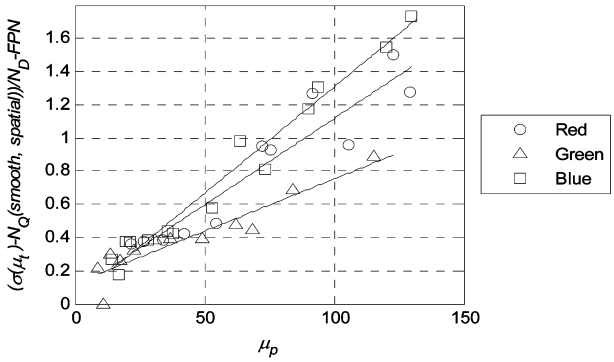

Fig. 5. Measured $PRNU$ for the i400 camera.

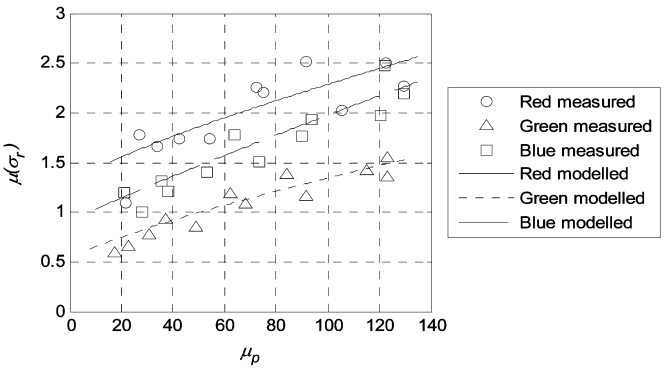

Fig. 6. Measured i400 camera noise and the predicted noise curve from the calibrated noise model.

The amplitude of $PRNU$ for a particular irradiance can be calculated by subtracting N_Q from (15), dividing by N_D, and subtracting FPN. Fig. 5 shows the measured $PRNU$ for the i400 camera, which increases approximately linearly with pixel value. $PRNU$ noise for the sensor is defined as the best-fit line for $PRNU$ noise values

$$\begin{aligned} PRNU_R &= 0.0104\mu_{p,R} + 0.0746 \\ PRNU_G &= 0.0063\mu_{p,G} + 0.1222 \\ PRNU_B &= 0.0128\mu_{p,B} + 0.0235. \end{aligned} \tag{16}$$

E. Row/Column Effects

The row and column noise for the i400 were measured and showed very little row or column noise dependence.

VI. Camera Model Calibration

The derived camera noise model in (1) was calibrated from the measured data in Sections IV and V, where sensor irradiance becomes a function of measured pixel value. Fig. 6 shows measured total image noise, and noise curves generated from the calibrated noise model. The values of total image noise $\mu(\sigma_r)$ and $\mu(\sigma_c)$ are highly correlated, hence only the row analysis is shown. The overall noise results illustrate a reasonable fit between the measured and modeled data. Maximum values for μ_p are restricted to 130 as this was the maximum value the i400 camera would output on the green channel when all digital effects were disabled or set to neutral.

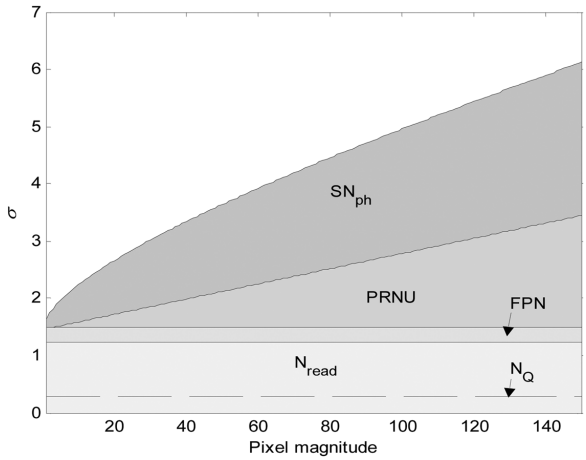

Fig. 7. Relative value of noise components for the blue channel of the i400 CCD camera at 22 °C environmental temperature. N_Q denotes the maximum potential quantization noise value, and $SN_{\rm dark}$ is zero.

Fig. 7 shows the relative magnitudes of the individually measured noise components on the blue channel for the i400 camera. N_Q represents the maximum potential contribution of quantization noise to overall noise and is dependent only upon final image content. Demosaicing noise is a scaling factor and is not included in the graph, and $SN_{\rm dark}$ is insignificant and is not shown as a contributor to noise. Image noise for this camera is clearly dominated by $N_{\rm read}$, $PRNU$, and $SN_{\rm ph}$.

VII. Discussion

The technique developed for measuring CCD noise has been validated on the i400 camera showing good correlation between the modeled and measured noise, although the green channel exhibits significantly lower noise and variation compared to the red and blue channels. This result is not unexpected as the Bayer color filter array contains twice as many green elements as each of red and blue. There is no reason to believe the technique for noise measurement will not hold for other CCD video cameras, although digital video cameras using non-CCD sensor types may require different noise models due to additional noise sources (e.g., active-pixel noise sources in CMOS imaging sensors).

VIII. Conclusion

A technique for measuring noise in a CCD video-camera has been developed that includes noise sources from the CCD and supporting ICs, color processing, and quantization. The noise components were grouped into measurable quantities and measured on a commercially available CCD camera. The derived CCD noise model was then calibrated with the measured data, generating a noise response which was dependent only upon pixel value and temperature. The modeled response compares favorably with measured total image noise.

The noise information gathered by the technique can be used in image processing applications to tune an algorithm to a particular image or images from a digital CCD video camera. For example an edge-detection algorithm could benefit from knowledge of the spatial noise content, or an object tracking function could utilize knowledge of the temporal noise to improve its reliability. A natural application for this technique is in the design of noise removal filters for images and video, where *a priori* knowledge of noise content could increase accuracy and robustness.

Analysis of camera noise from the image alone can provide a good estimate of image noise, although care should be taken as the image noise is heavily dependent upon its content.

References

[1] J. Nakamura, *Image Sensors and Signal Processing for Digital Still Cameras*. Boca Raton, FL: CRC Press, 2006.
[2] A. E. Gamal and H. Eltoukhy, "CMOS image sensors," *IEEE Circuits Devices Mag.*, vol. 21, no. 3, pp. 6–20, May/Jun. 2005.
[3] G. E. Healey and R. Kondepudy, "Radiometric CCD camera calibration and noise estimation," *IEEE Trans. Pattern Anal. Mach. Intell.*, vol. 16, no. 3, pp. 267–276, Mar. 1994.
[4] H. W. Ott, *Noise Reduction Techniques in Electronic Systems*, Second ed. New York: Wiley, 1988.
[5] R. A. Boie and I. J. Cox, "An analysis of camera noise," *IEEE Trans. Pattern Anal. Mach. Intell.*, vol. 14, no. 6, pp. 671–674, Jun. 1992.
[6] H. Tian, B. Fowler, and A. E. Gamal, "Analysis of temporal noise in CMOS photodiode active pixel sensor," *IEEE J. Solid-State Circuits*, vol. 36, no. 1, pp. 92–101, Jan. 2001.
[7] Y. Tsin, V. Ramesh, and T. Kanade, "Statistical calibration of CCD imaging process," in *Proc. IEEE 8th Int. Conf. Computer Vision*, 2001, vol. 1, pp. 480–487.
[8] "Noise analysis in operational amplifier circuits," in *Digital Signal Processing Solutions SLVA043A*, 1999.
[9] G. K. Bhattacharyya and R. A. Johnson, *Statistical Concepts and Methods*. New York: Wiley, 1977.
[10] H. Baher, *Analog and Digital Signal Procesing*. New York: Wiley, 1990.
[11] R. Ramanath, W. E. Snyder, and G. L. Bilbro, "Demosaicking methods for Bayer color arrays," *J. Electron. Imag.*, vol. 11, pp. 306–315, 2002.